HUNGARIAN UNIVERSITY OF AGRICULTURE
AND LIFE SCIENCES

Modelling and optimization of large-scale grid-connected photovoltaic systems with enabling technologies

DOI: 10.54598/007220

PhD Dissertation

by

Teklebrhan Tuemzghi Negash

Gödöllő
2025

Doctoral school and program denomination:

Doctoral School of Engineering Sciences

Doctoral Program of Mechanical Engineering

Science: Engineering

Head of School: Prof. Dr. László Bozó, MHAS
Institute of Environmental Sciences
Hungarian University of Agriculture and Life Science, Budapest, Hungary

Program leader: Prof. Dr. Gábor Kalácska, DSc
Institute of Technology
Hungarian University of Agriculture and Life Science, Gödöllő, Hungary

Supervisor: Prof. Dr. István Farkas, DSc
Institute of Technology
Hungarian University of Agriculture and Life Science, Gödöllő, Hungary

Co-Supervisor: Dr. István Seres, PhD
Institute of Mathematics and Basic Sciences
Hungarian University of Agriculture and Life Science, Gödöllő, Hungary

…… ……

Affirmation of supervisor(s) Affirmation of head of doctoral program

CONTENTS

1. INTRODUCTION, OBJECTIVES

The deployment of solar photovoltaic (PV) systems, covering both large utility-scale and small residential installations, has been increasing rapidly worldwide. Forecasts show that utility-scale PV installations will account for approximately 66.7% of the global energy mix by 2050. Similarly, the adoption and utilization of residential PV are skyrocketing, as buildings, once primary energy consumers, have become energy producers. Declining costs of home batteries and PV components are driving consumers to generate their own power locally, reducing their grid reliance. However, extensive deployment of these resources challenges the grid, as large-scale integration requires complex system adaptations. Key issues include intermittency, matching, forecast uncertainty, adequacy, and grid stability. To overcome these challenges, various solutions have been proposed in the literature, including energy storage, resource complementarity, curtailment, resource diversity, and advanced forecasting.

In the context of large-scale PV integration, it is crucial to evaluate the combined impact of multiple enabling tools, including the PV-wind mix, storage capacity and duration, curtailment strategies, and balancing requirements. Considering these factors together provides a more comprehensive understanding of system design and operation, as focusing on PV alone fails to capture the full complexity and interdependencies inherent in modern power system dynamics. A well-balanced PV-wind mix can increase RE penetration while reducing storage and curtailment compared to standalone PV systems. Integrating large-scale PV requires diverse energy storage solutions, which are essential for enhancing grid flexibility, increasing renewable penetration, and accelerating the transition to 100% RE.

Understanding how penetration, storage capacity and duration, curtailment, PV-wind mix, and balancing requirements interact provides key insights for managing the transition to a renewable-dominated grid and anticipating its operational requirements. However, empirical data showing the interaction between these parameters with sufficient detail does not exist. The majority of the current energy transition studies are primarily driven by least-cost optimization (techno-economic) models, often overlooking these critical technical factors in favour of extensive economic data. This work, therefore, aims to develop a flexible modelling framework that assesses interactions among key system design parameters and supports optimized PV integration while leveraging the benefits of residential PV and advanced PV generation forecasting and optimization.

The primary objectives of this research are to:

- Maximize the share of PV in the electricity grid with high reliability and operational efficiency, contributing to a sustainable energy system;
- Investigate the complex interaction among the various system design parameters, such as PV-wind mix, storage capacity and duration, curtailment strategies, and balancing requirements, and their impact on system design and performance;
- Formulate a relationship among the major design parameters and system efficiency, supported by robust empirical data, to develop practical guidelines for achieving high levels of renewable integration.
- Enhance the contribution of residential PV on the power mix by exploring the impact of feed-in constraints on promoting higher local consumption of residential PV in low-voltage local networks;
- Leverage machine learning-based PV generation forecasting to enhance real-time operational management and optimization of PV systems, mitigating uncertainties and limitations inherent in the design phase of PV integration.

2. MATERIALS AND METHODS

This chapter provides a comprehensive explanation of the materials, techniques, and equipment utilized.

2.1. PV integration modelling

The study is conducted in Eritrea, North East Africa, located in the arid and semi-arid regions of the Sahel region in Africa at a latitude between 12 ° 22′ and 18° 02′ N and a longitude between 36° 26′ and 43° 13′ E.

Data for this study were sourced from multiple sources. Solar irradiation and wind speed data from Ministry of Energy and Mines, Eritrea, supplemented with data from Photovoltaic Geographical Information System (PVGIS) and the Global Wind Atlas (GWA), and load data from Ethiopia, along with experimental data.

The wind and solar generation capacity are evenly distributed between the six locations, with the total generation normalized to a peak capacity of 1 MW.

The generation mix at each hour of the year is calculated according to:

$$P_{\text{rew}}(t) = p\ \alpha(r)\ (r\ p_{\text{PV}}(t) + (1-r)\ p_{\text{wind}}(t)),$$

where t is a time step, $p_{\text{PV}}(t)$ is the PV production, $p_{\text{wind}}(t)$ is the wind turbine generation, r is the PV ratio, p is the minimum no-dump capacity (in MWp). And $\alpha(r)$ is a factor that is determined from a requirement that:

$$\sum_t \alpha(r)(r\ p_{\text{PV}}(t) + (1-r)\ p_{\text{wind}}(t)) = \text{const},$$

and that $\alpha(0.5) = 1$.

The net load (P_{mix}), the mismatch between renewable generation and load can be computed as:

$$P_{\text{mix}}(t) = \beta\ P_{\text{nd}}\ \alpha(r)\ \left(r\ p_{\text{PV}}(t) + (1-r)\ p_{\text{wind}}(t)\right) - P_{\text{load}}(t),$$

where β is a multiplier that enables oversizing the generation.

2.2. Storage modelling

Based on the generation mix (P_{mix}), the storage is modelled according to:

$$S(t) = \begin{cases} S(t-\Delta t) + \min\left(\eta_{\text{ch}}\ P_{\text{mix}}(t), P_{\text{room\_d}}(\text{t})\right)\ \Delta t, & \text{if } P_{\text{mix}} \geq 0 \\ S(t-\Delta t) + \min\left(\frac{P_{\text{mix}}(t)}{\eta_{\text{dis}}}, P_{\text{room\_d}}(\text{t})\right)\Delta t\ , & \text{if } P_{\text{mix}} < 0 \end{cases}$$

$$\forall \text{t} \in\ |1, N|\ , \text{and}\ \ \text{S}(0) = 0$$

where $\text{S}(t)$ is the stored energy (MWh) at time $t, \Delta\ t = 1$ h is the time step, N is the number of hours in a normal year, 8760, and $P_{\text{room\_d}}\Delta t$ is the hourly remaining capacity of storage during charging and discharging.

Seasonal storage is introduced when penetration surpasses 80% curtailment (E_p) is greater or equal to 5%.

Seasonal storage S_h at each hour of the year is computed according to

$$S_h(t) = \begin{cases} S_h(t-\Delta t) + \min\left(\eta_{\text{ch\_s}}\, E_{\text{p}}(t), P_{\text{room\_s}}(\text{t})\right)\Delta t, & \text{if } P_{\text{mix}} \geq 0 \\ S_h(t-\Delta t) - \min\left(\frac{P_{\text{u}}(t)}{\eta_{\text{dis\_s}}}, -P_{\text{room\_s}}(\text{t})\right)\Delta t\,, & \text{if } P_{\text{mix}} < 0 \end{cases}$$

where: S_{maxh} is the maximum capacity of the hydrogen storage (seasonal storage), $\eta_{\text{ch\_s}}$ is the electrolyser efficiency, $\eta_{\text{dis\_s}}$ is fuel cell efficiency, and $P_{\text{room\_s}}$ is the available capacity at each hour

Renewable penetration (P) is computed according.

$$\text{P} = \frac{\sum P_{\text{con}}\,\Delta t}{\sum P_{\text{load}}\,\Delta t}, \quad \text{where } P_{\text{con}}(t) \text{ is the total consumed RE}$$

The balancing capacity (unmet demand, P_{BC}) needed can be computed:

$$P_{\text{BC}}(t) = -P_{\text{mix}}(t) - \min(-P_{\text{mix}}(t)\,, -\eta_{\text{dis}} P_{\text{room}}(t)),$$

The two newly introduced are:

The two newly introduced indices are computed according to:

Storage utilization (SU)

$$SU = \frac{-\sum(S(t)-S(t-\Delta t))}{S_{max}}, \qquad \text{if } \; S(t) < S(t-\Delta t)$$

System-use index (SUI) is computed as follows:

$$\text{SUI} = \text{SU} \times k \times m \times u$$

where: $k, m \; and \; u$ – are calculated by dividing annual energy discharge by the total consumed RE, average charging power by power capacity (PC), and total consumed RE by total RE generation, respectively:

This study examines the impact of complementarity on system performance by creating various solar and wind mix, from which PV ratio of 0%, 50%, and 100% of the total renewable generation.

2.3. Residential PV integration

For maximizing the integration of direct consumption of residential PV a simplified algorithm shown in Fig.1 is employed.

At the distribution side of the network, the following dispatch algorithms are computed at each time step:

The power that is directly fed (P_{inj}) to the grid at a time, t is:

$$P_{\text{inj}}(t) = \min\left(\; P_{\text{gen}}(t), P_{\text{limit}}\right),$$

where: P_{gen} is the generated PV power at time t and P_{limit} is the injection limit.

The battery energy storage (BES) is modelled with charging and discharging efficiencies ($\eta_{\text{ch}} = \eta_{\text{dis}} = \sqrt{0.9}$), according to

$$\text{BES}(t) = \text{BES}(t-1) + \min\left(\eta_{\text{ch}}\,(P_{\text{excess}}(t), P_{\text{room}}(\text{t}))\right)\Delta t \; - P_{\text{bat,inj}}(t),$$

Where, P_{excess} is the excess generation above the feed-in limit and P_{room} is the remaining capacity, $P_{\text{bat,inj}}$ denotes the constant night-time battery discharge and BES_{max} is battery rated capacity.

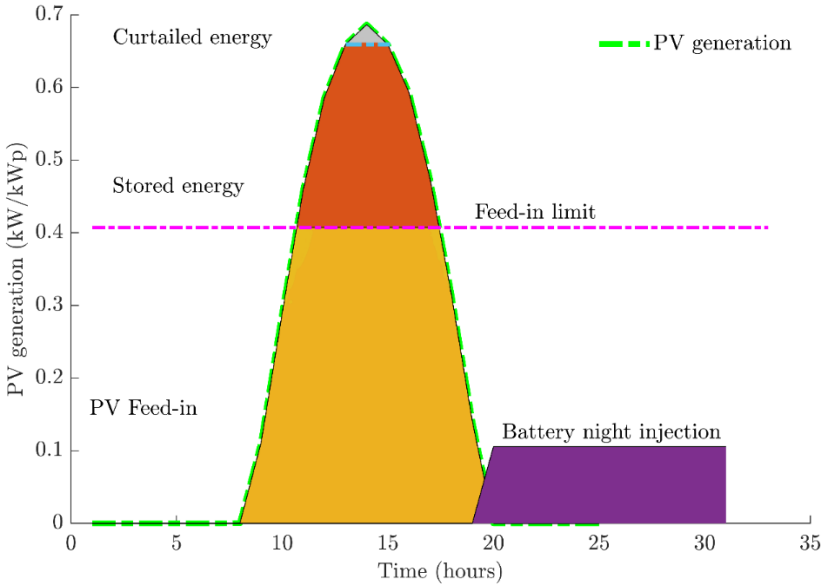

Fig. 1. An illustrative diagram showing the PV-battery dispatch strategy in the proposed method, with a feed-in limit applied (for June 1st)

2.4. PV power generation forecasting

Renewable forecasting is crucial for balancing the grid system and enhancing operational performance. Fig. 2 provides the general schematic diagram of the methodological approach followed in this section.

The study utilizes 17 years of hourly weather data from the PVGIS data assimilation platform, along with one year of measured data from the actual plant, to develop a forecasting model for predicting hours ahead of PV power generation. Two engineered features were introduced to help the models capture seasonal and time-related patterns: the sine and cosine transformations of the timestamp.

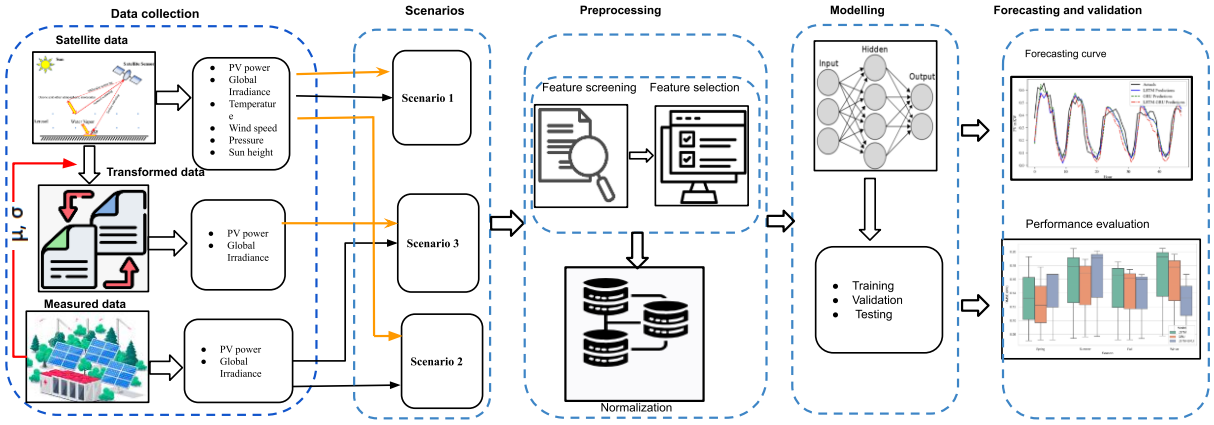

Fig. 2. Graphical abstract of the proposed methodological approach followed

This study explores several deep learning models for accurate PV power forecasting, including LSTM, GRU, (XGBoost) and SARIMAX, as well as advanced models such as CNN, TCN, and transformers and their hybrids by developing three different scenarios. We employed a modified version of the Z-score transformation to align satellite-derived solar data with ground-based measurements by linking the mean and standard deviation of both datasets. For each

value in satellite-derived data, we find the standard normal form using the Z-score transformation (z).

$$z = \frac{P_{sat,i} - \mu_{sat}}{\sigma_{sat}}$$

The rescaled value ($P'_{sat,i}$) is computed to match the distribution of the measured data using:

$$P'_{sat,i} = z * \sigma_{meas} + \mu_{meas}$$

where: $P_{sat,i}$ is satellite-derived hourly PV generation, μ_{sat} is mean of the satellite-derived data, σ_{sat} is the standard deviation of the satellite-derived data, μ_{meas} is the mean of the measured data, and σ_{meas} standard deviation of the measured data.

Reinforcement Learning (RL), RL is used to optimize battery dispatch in PV integration. The agent learns to manage energy flows-charging, discharging, and curtailment-based on hourly PV and wind generation and load demand.

2.5. Experimental setup for power quality analysis

The experiment was conducted in the Szent István Campus (coordinates 47°35′40.7″N and 19°21′42.3″E), at the grid-connected PV system located in front of the Aula building. Measurements were taken at the point of common coupling, where the transparent glass modules of the monocrystalline Si connected to the grid through the SolarEdge inverter. Connectors were installed to safely facilitate measurements using a standard power quality analyser, the Wally 'A' Power Quality Analyzer as shown in Fig 3. The PV system, with a total capacity of 3.3 kW, is installed at an inclination of 40^0 and an azimuth of $180^{0,}$ directly facing south. The specification of the PV system and inverter is given in Appendix A7. Fig. 3.4 shows the complete set of measurement setups.

Measurements were conducted on October 12 and 13, 2025, under partly sunny conditions. These dates were deliberately selected to assess the impact of varying weather conditions on power quality.

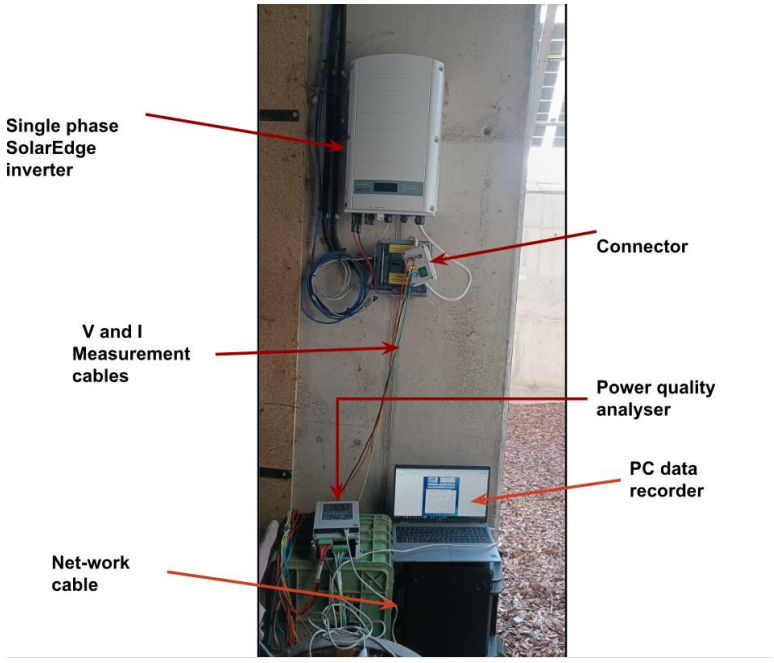

Fig. 3. Power quality analyser measurement setup

3. RESULTS AND DISCUSSION

This chapter presents the detailed results of the newly developed methodological framework for integrating large-scale PV, which aligns with the thesis objective.

3.1. Generation and demand variability

Fig. 4 illustrates how mismatch power varies with changes in the PV fraction when RE-to-load ratio of 1 is applied. The vertical axis represents the frequency, indicating the number of hours within each 100 MW mismatch interval.

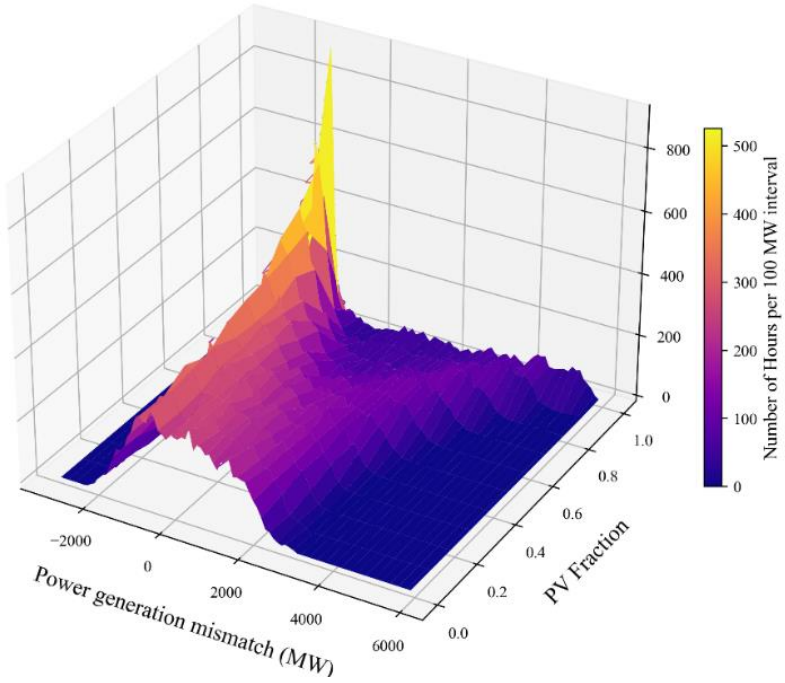

Fig. 4. Variable generation mismatch as a function of PV fraction and frequency

Understanding these variabilities is crucial for designing a system that addresses all the uncertainties of a VRE-dominated grid. The optimum ratio should have high frequency at lower mismatch or low frequency at higher mismatch.

Table 1 outlines the key components of selected renewable energy scenarios designed to study system design issues and associated performance.

Table 1. Description of the different scenarios analysed

Scenarios Names	Solar share (%)	Wind share (%)	Hours of storage	Storage technology
Solar only	100	0	1,2,4,6,8,10	Li-ion battery
50-50 scenario	50	50	1,2,4,6,8,10	Li-ion battery
Wind only	0	100	1,2,4,6,8,10	Li-ion battery

3.2. Renewable use without storage

For mathematical simplicity and reference, the analysis starts with determining the no-dump capacity, the threshold above which the system requires storage or curtailment or both. The

lowest no-dump capacity occurs in the wind-only scenario (100% wind), while the highest is observed in the 100% PV ratio (solar-only scenario).

Fig. 5 shows the penetration and curtailment for different PV-wind mix when no storage is employed. A wind-dominated mix achieves higher penetration across all RE-to-load ratios and thus experiences lower curtailment. The maximum penetration, even though the gain over the wind-only scenario was small, is reached at around 20-25% of the PV ratio when curtailment remains less than 30%.

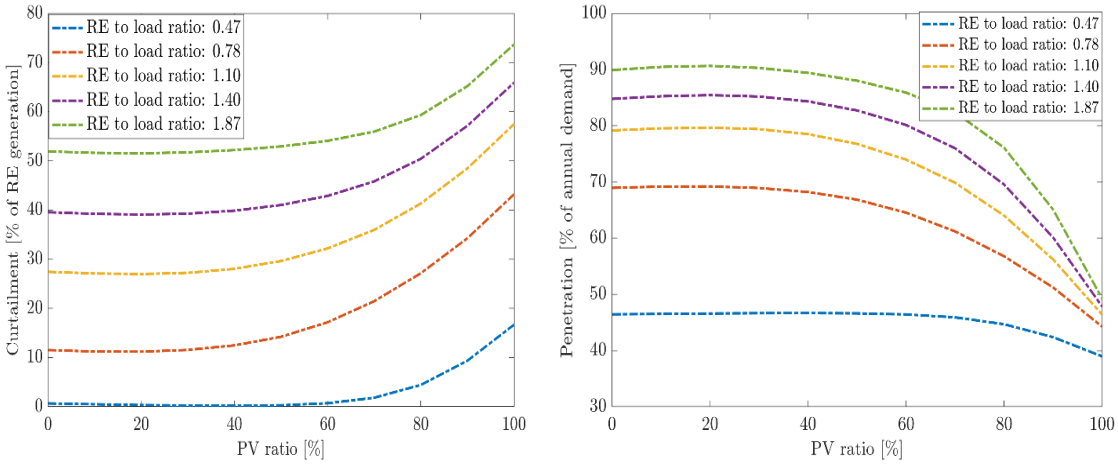

Fig. 5. Renewable energy a) penetration and b) curtailment as function PV ratio

3.3. Renewable use with energy storage application

Fig. 6 shows how the penetration and curtailment vary with varying PV–wind mixes at fixed storage capacity of 0.41 average daily demand. The impact of storage showed a marked difference as RE to load ratio increases to 1.1 at 0.41 average daily demand, where we already observe approximately 96% penetration for only 9% curtailment at 80% PV mix.

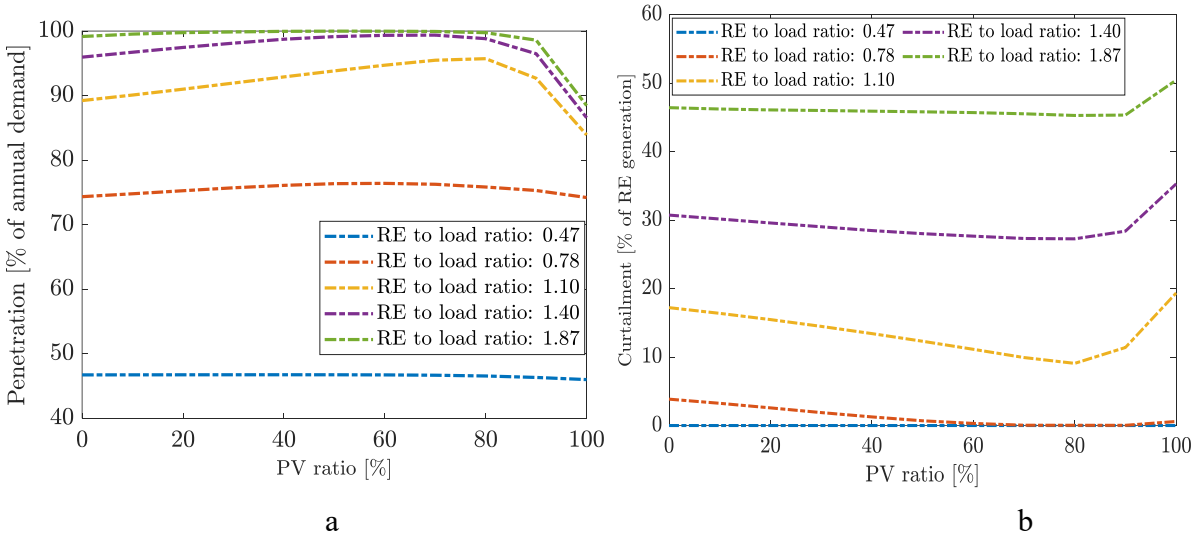

Fig. 6. Renewable energy: a) Penetration, b) Curtailment as a function PV ratio, with 0.41 of average daily demand

The interaction between VRE penetration, storage capacity, and curtailment is analysed for all scenarios. The effect of curtailment is more dominant in wind wind-only scenario, whereas in the solar-only scenario, the impact of storage surpasses that of curtailment. For the 50-50 PV-

wind scenario, however, penetration is the result of considerable effect of both storage and curtailment. The 50-50 PV-wind scenario demonstrates superior performance, allowing us to easily achieve a 90% penetration with reasonable storage and curtailment. The solar-only scenario shown in Fig. 7 shows a different pattern from the previous two scenarios, regardless of the generation capacity, the penetration remains low at lower storage capacities, with significant curtailment.

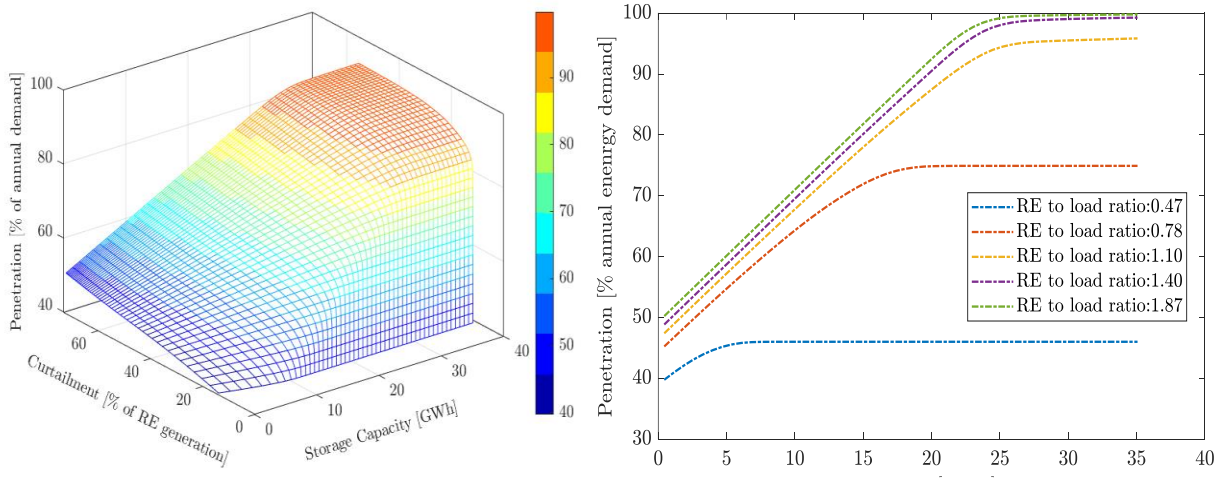

a b

Fig. 7. Solar-only scenario with 6 hours storage, interaction between, a) Penetration, curtailment, and storage capacity, b) Storage capacity and penetration

Diurnal storage is suitable up to 80-90% penetration level, beyond which seasonal storage becomes essential to mitigate seasonal fluctuation. Satisfying the final 10% demand requires significantly increased installed capacity and storage as shown in Fig. 8.

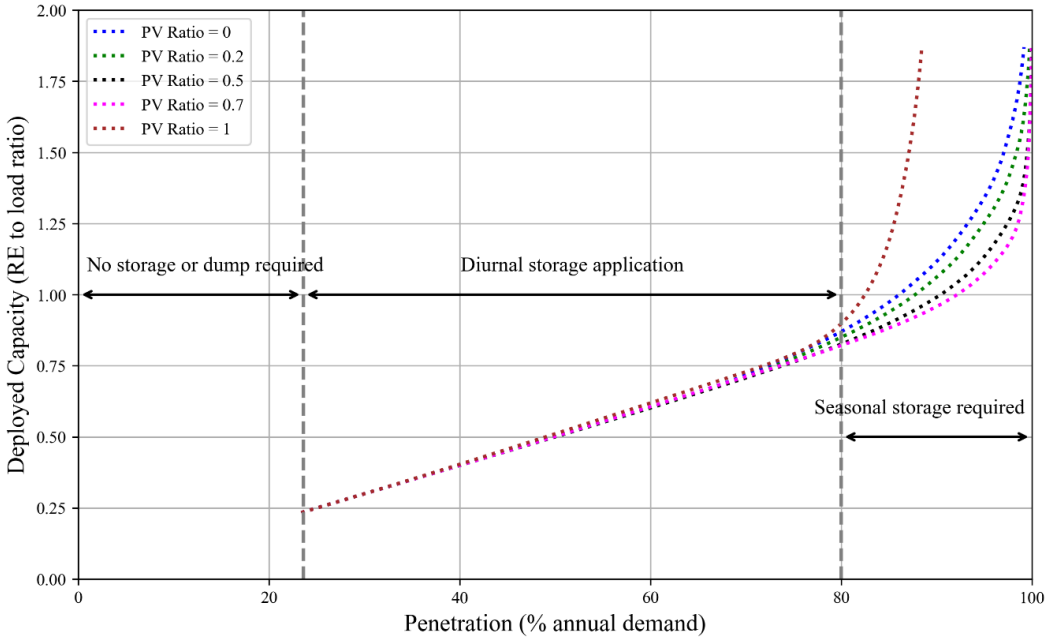

Fig. 8. Illustration of renewable energy requirements at different stages of renewable penetration

3.4. Storage utilization and system-use index

In this section, two new indices were introduced to identify optimal system design parameters. Fig. 9 shows that storage utilization is significantly high at low storage capacity, particularly for some suitable curtailment ranges. However, the utilization index decreases as the storage capacity increases. This observation suggests that deploying large storage for diurnal applications with wind energy may not be advisable due to the risk of underutilization. To address these limitations, we introduced a new index called the system-use index (SUI). This index provides a more comprehensive evaluation of system performance by linking storage utilization and RE consumption and generation with other factors, such as storage charging/discharging, and energy and power. System-use index offers deeper insights into how effectively storage is integrated within the broader energy system and its role in enhancing the system's ability to manage variability and optimize resource deployment. Fig.3.6b illustrates the system-use index for the wind-only scenario. The figure presents various combinations of storage and curtailment, along with their corresponding system-use index values.

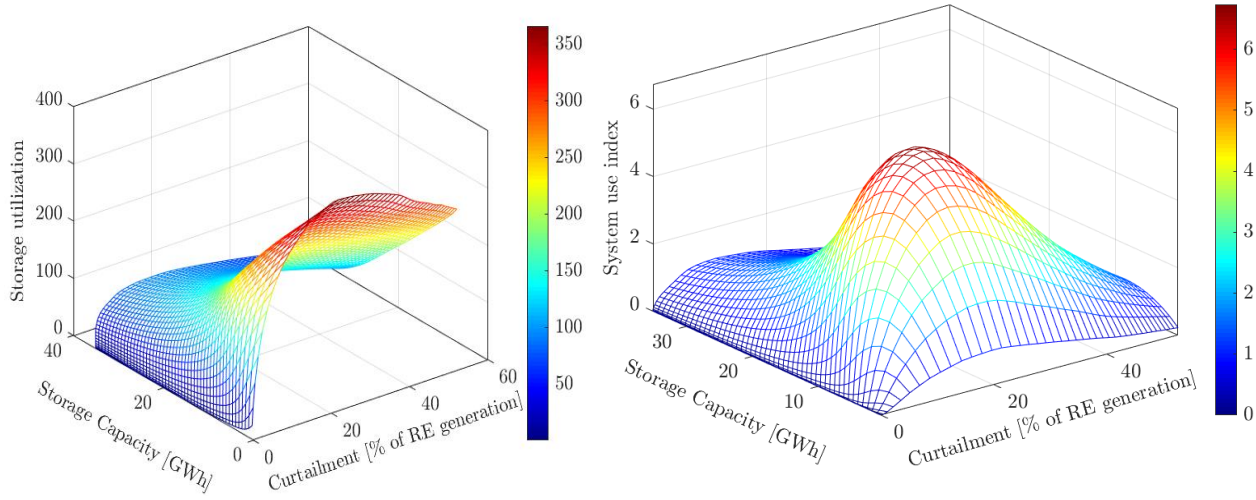

a b

Fig. 9. System performance indicators: a) Storage utilisation, b) System-use index for 50-50 wind-solar scenario at 6 hours of storage

The storage and curtailment combination that leads to the top plateau region of the system-use index represents the optimal values that effectively maximize the overall system performance. For example, the maximum system-use index value occurs at 8.9 GWh storage capacity and 16% curtailment at an RE-to-load ratio of 1.1. The Maximum system use index in solar and wind-only scenarios requires a higher storage and curtailment, respectively. Overall, it is worth noting that the graph in these figures builds a hill with a plateau top, showing several combinations with almost equal system benefits as shown in the contour plot Fig. 10.

Based on these results, I conclude that well-utilized storage capacity of approximately 0.2 of average daily demand, coupled with a reasonable curtailment of 16%, can effectively achieve a penetration target of 90%.

The observed SUI value increases (discussed in reference to the peak plateau region of each plot) when we increase hours of storage from 1h to 6h, showing that hours of storage value impacts system role of the storage. Beyond 6h, SUI gradually decreases. The small decrease may be because the high storage hours (like 10 h) allow the system some seasonal role in combination with curtailment. Fig. 11 presents SUI values for 2h, 6h and 10h storage for 50-50 PV-wind scenario.

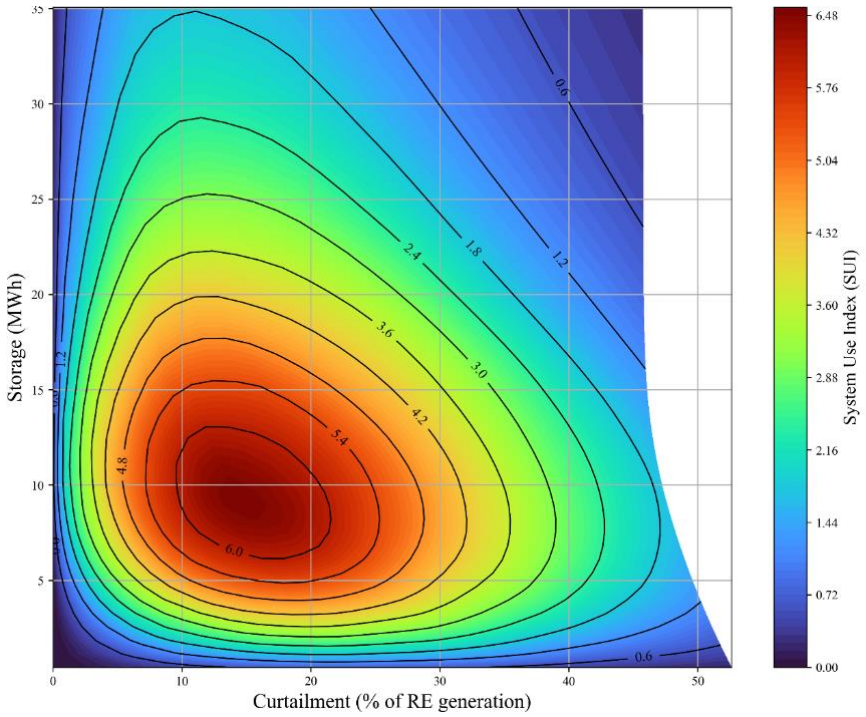

Fig. 10. Contour plot of the System Use Index (SUI) across a range of storage capacities and curtailment levels for 50-50 PV–wind Scenario

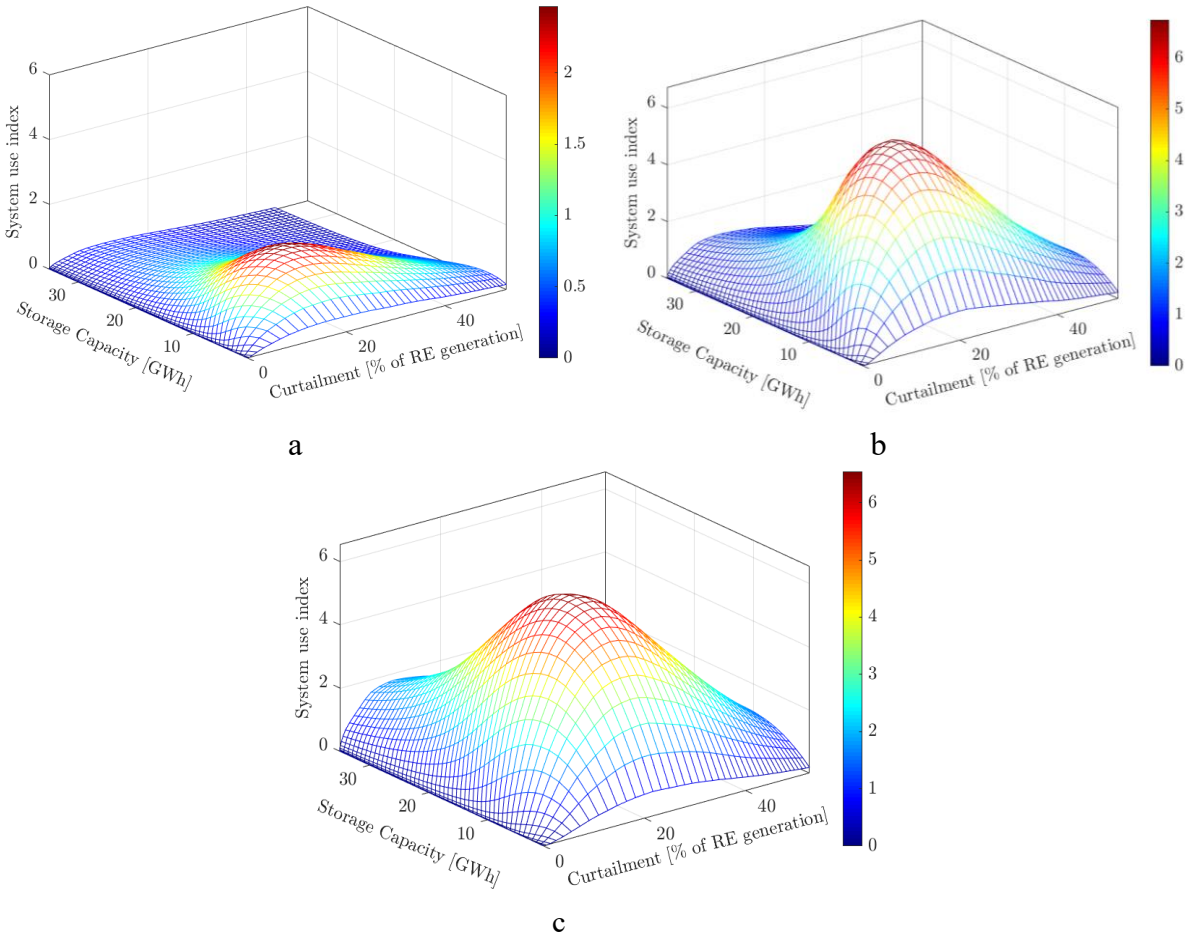

Fig. 11. System–use index: a) 2 hours, b) 6 hours, c) 10 hours

3.5. Seasonal storage application for seasonal mismatch

Fig. 12 illustrates the penetration levels achieved when seasonal storage, along with diurnal storage with a 6-hour duration, is applied across the three scenarios analysed at a RE-to-load ratio of 1.3. When seasonal storage is applied penetration reaches approximately 100% and 98% at 180 GWh (equivalent to 4 average daily demand) for the 50-50 and wind-only scenarios, respectively. In contrast, the solar-only scenario requires a larger storage capacity to achieve the same penetration level. In this scenario, increasing diurnal storage from 0.16 to 0.5 average daily demand (3.12b) enables 100% penetration at significantly reduced seasonal storage.

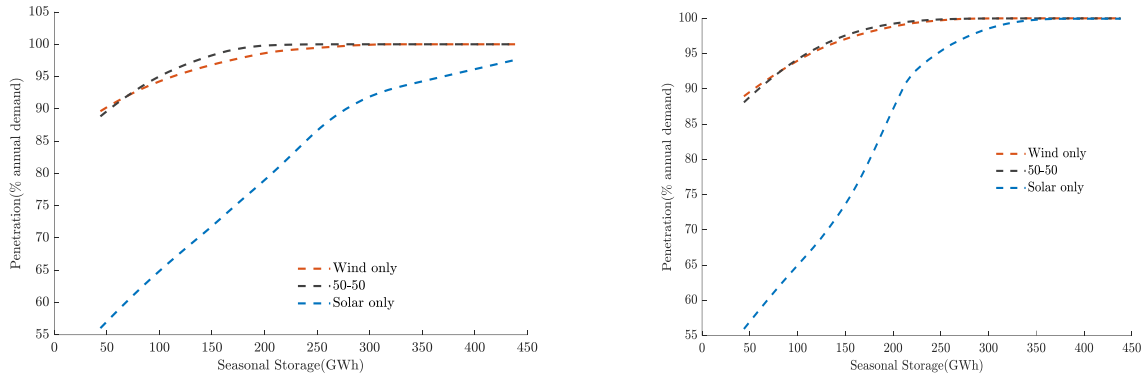

Fig. 12. RE penetration using seasonal storage combined with diurnal storage of capacities: a) 0.16, b) 0.5 times the average daily demand

3.6. Dispatchable balancing requirements

Fig. 13 shows the contribution of all system input variables, including balancing generators and curtailed energy, over the first week of January (50-50 PV–wind scenario, with a 1.1 RE-to-load ratio and storage capacity equal to 0.41 times the average daily demand). The balancing requirement required for balancing the system reaches up to 80% of the peak load.

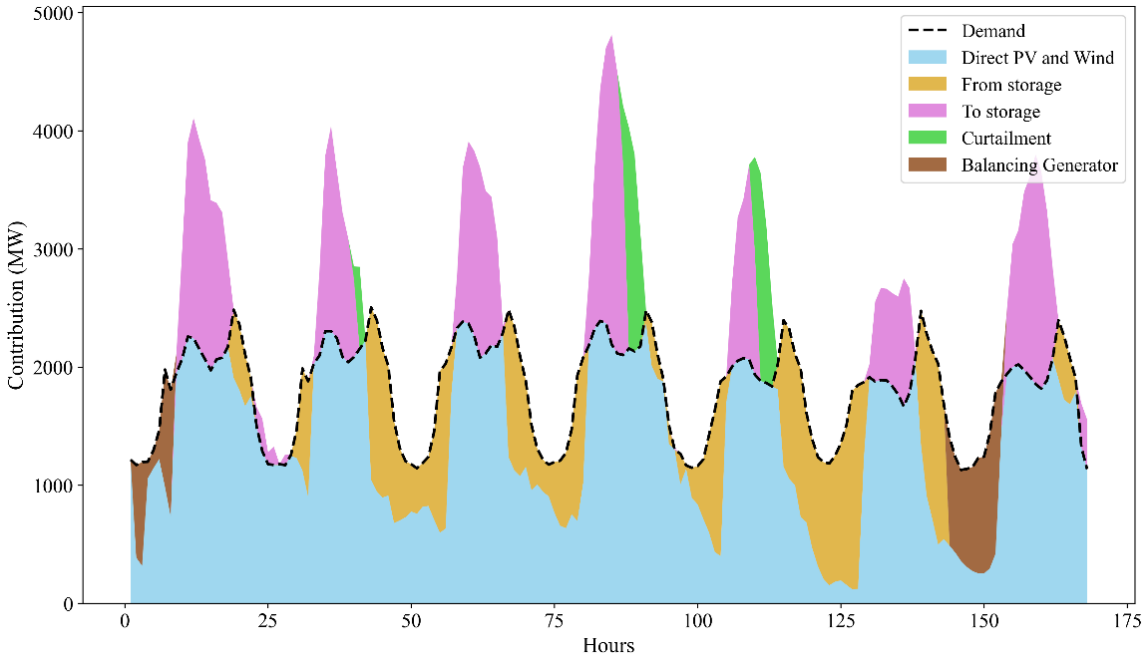

Fig. 13. Contribution of all deployed technologies in meeting the demand

3.7. Evaluating the potential of residential PV integration

The contribution of residential PV to overall renewable integration is quantified by evaluating its share in meeting national electricity demand under varying feed-in limits. The annual generated power increases with the feed-in limit, peaking when all generated energy is directly injected into the grid at a limit of 0.8 kW/kWp and above (Fig. 14).

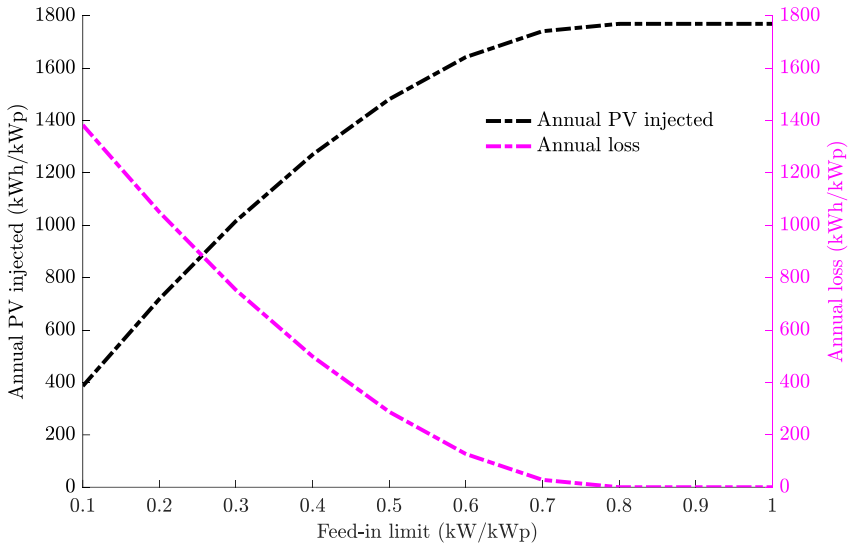

Fig. 14. Annual average energy generation and energy loss for varying feed-in limit

Allowing a high feed-in limit increases penetration and decreases losses; however, it can lead to an excess of generation over consumption in the local network, resulting in reverse power flow. Feed-in limit above 0.7 kW/kWp demonstrates a negligible impact as shown in the figure.

At the ideal feed-in limit, almost all energy rejected from the grid due to feed-in constraints is stored in the battery for nighttime use. Consequently, battery storage below 2 kWh/kWp is found sufficient enough to maximize the overall system performance when fitted with this ideal feed-in limit, as shown in Fig. 15.

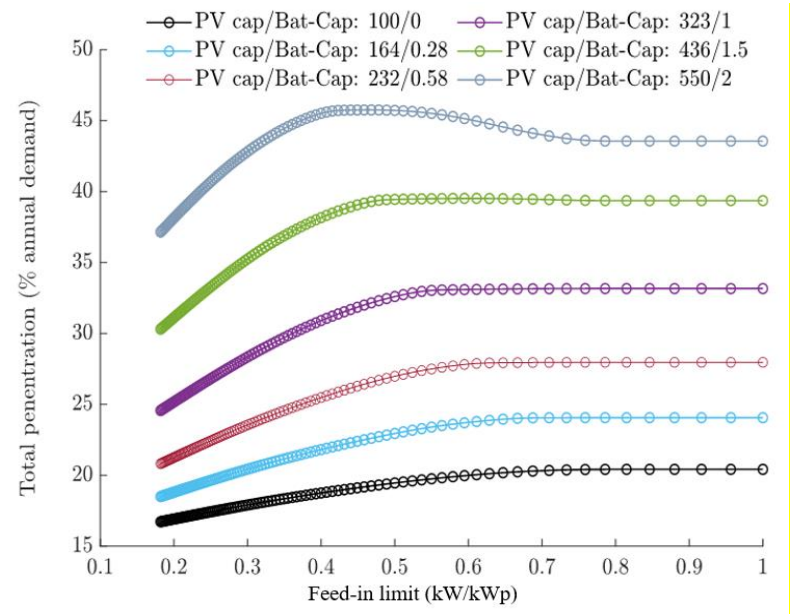

Fig. 15. Penetration as function of Feed-in limit for different pairs of PV capacity and battery sizes

3.8. Power quality issues in grid-connected PV systems

In this section, experimental data is analysed focusing on selected parameters – active power output, current total harmonic distortion (ThdI), voltage total harmonic distortion (ThdV), and voltage deviation (V_Dev) – measured at 3-second intervals to examine the impact of the temporal variability of weather conditions on PV power output and its quality.

Fig.16 presents the active power output normalized to its peak capacity of 3.3 kW. The plot shows a gradual increase in power output from morning until noon, followed by a decline in the afternoon, and remains zero in the night hours. The maximum PV output recorded was approximately 0.72 kW/kWp, corresponding to the normalized peak capacity (P/P_{rated}). This shows that there are a few hours in the year when power generation is above 0.72 kW/kWp and this offers insignificant benefit to the system in increasing the aggregate annual generation. This aligns closely with the findings in Section 4.2.1, which indicate that applying a feed-in limit above 0.7 kW/kWp yields negligible gains in annual energy generation.

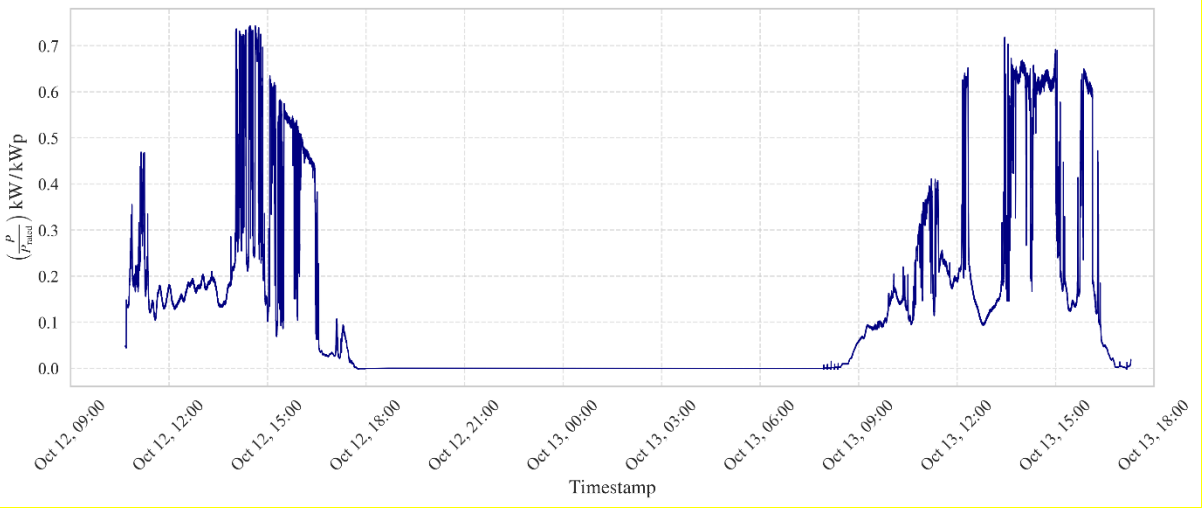

Fig. 16. The active PV power out as normalized to its peak capacity 3.3 kWp

To investigate the total harmonic characteristics of the PV inverter at various operating conditions of power generation, the generated power relative to its rated capacity (P/P_r) is divided into three categories: lightly loaded inverter (0-0.3), medium loaded inverter (0.31 - 0.5), and heavily loaded inverter (0.51- 0.74). The current harmonic distortion exhibits a strong correlation with inverter loading; however, the data provides limited evidence on how voltage harmonic distortion is affected by inverter loading.

Fig. 17 illustrates the relationship between current total harmonic distortion (ThdI) and active power. The figure shows a strong correlation between the two parameters. This indicates that inverter loading has a greater impact on ThdI than on the other power quality indicators, such as ThdV and voltage deviation. In heavily loaded inverters, ThdI remains relatively low, with only a few points exceeding the permissible limit of 5%. However, as the inverter load decreases, ThdI gradually exceeds this limit and rises further, reaching values of around 10%. The change in ThdI becomes more pronounced under lightly loaded conditions. This suggests that inverter loading plays a decisive role in the injection of current harmonics into the grid, with a strong caution that lightly loaded (underutilized) inverters contribute significant waveform distortion.

A cubic polynomial function fits the curve well, achieving an R^2 value of 0.926. At higher loading levels, inverter behaviour becomes more stable, likely because MPPT and control mechanisms operate more actively and consistently when PV generation is higher. These results highlight the importance of designing inverters that maintain robust control and predictable power-quality performance across a wide range of loading conditions.

Accordingly, the total current harmonic distortion (y) as a function of active power (x) of the three inverter loading categories can be reliably estimated using a single cubic polynomial model:

$$y = 1.3546 + (-0.2973)\,x + (0.0239)\,x^2 + (-0.00063)\,x^3$$

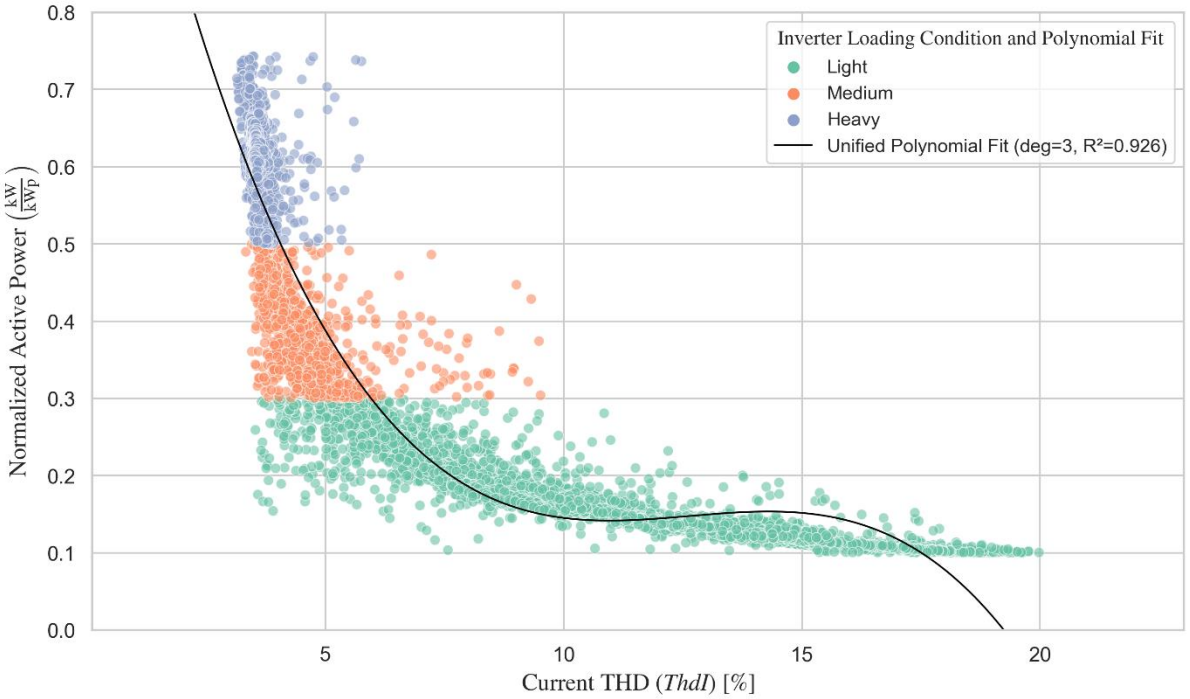

Fig. 17. Active power versus total harmonic distortion under different loading conditions

The greater variation in ThdI observed in lightly loaded inverters implies that they are more sensitive to harmonic distortion when underutilized. Lightly and medium-loaded inverters exhibit higher variability per unit change in active power, whereas heavily loaded inverters show less variability. By associating these distinct regression behaviours with specific sites, utilities can tailor inverter deployment strategies and better anticipate grid stress based on localized loading profiles.

This suggests that inverter behaviour becomes more stable at higher loading levels, likely due to more effective control operation under these conditions. Consequently, oversizing an inverter for a given design can negatively impact power quality – not only cost – because an oversized inverter tends to operate predominantly under medium or light loading, where harmonic distortion is more pronounced. These findings highlight the need for inverter designs that ensure stronger control capability and more predictable interactions among power-quality parameters across varying load conditions.

3.9. Advancing large-scale PV integration with accurate forecasting

In this section an improved forecasting model is proposed to maximize PV penetration. The performance of various models (LSTM, GRU, CNN, XG Boost, SARIMAX, TCN, and informer and their hybrid) in predicting uni-step and multi-step PV generation is compared by developing different scenarios. To address the data scarcity challenges, a modified Z-score transformation was introduced. The results demonstrate a significant improvement compared to those obtained without the modified Z-score transformation. The findings further reveal that the proposed transformation improves forecasting accuracy by up to 24% in LSTM-GRU and 29.4% for Informer in six-step prediction, based on RMSE. Such improved forecasting enhances grid stability, optimizes energy dispatch, and offers a scalable solution for regions with limited measurement infrastructure. Fig. 3.15 showed the performance comparison of the selected models.

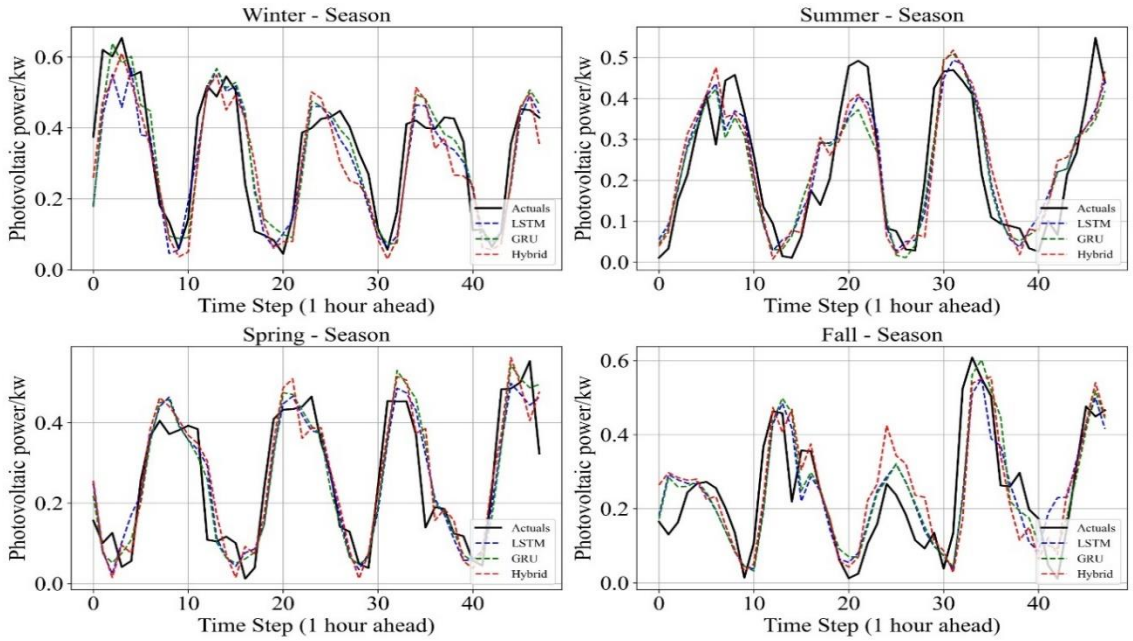

Fig. 3.15. Performance comparison of the three models' prediction of actual PV generation across four seasons in 1-step prediction horizons

The study demonstrates that satellite-trained models effectively predict PV generation, overcoming data scarcity issues by utilizing extensive satellite datasets. The findings show the importance of considering weather variability for reliable forecasting, especially in multi-step predictions, which are vital for long-term renewable energy planning. Moreover, the RL-based optimization showed an improved performance compared to the rule-based approach, demonstrating its capability in optimizing renewable integration.

4. NEW SCIENTIFIC RESULTS

This section presents the new scientific findings from this research work as follows:

1. A methodological approach for integrating large-scale PV

I have introduced a novel methodological framework aimed at maximizing PV penetration in the power grid. This approach systematically examines the interplay between key system design parameters and overall efficiency by varying these parameters to generate diverse operational scenarios and assess their sensitivities. For the first time, it explicitly incorporates the interactions among critical factors–such as PV–wind mix, storage capacity, storage duration, penetration level, curtailment, and balancing capacity needs–across a wide range of scenarios, thereby providing deeper insights into system design and performance.

The methodological framework I developed, which is the basis for designing and modelling the system with all its interacting system parameters, is presented as follows:

The different mixes of solar PV and wind-generated power can be computed by:

$$P_{\text{rew}}(t) = P_{\text{nd}}\, \alpha(r)\, (r\, p_{\text{PV}}(t) + (1-r)\, p_{\text{wind}}(t)),$$

$\alpha(r)$ is a factor that is determined from a requirement that:

$$\sum_t \alpha(r)(r\, p_{\text{PV}}(t) + (1-r)\, p_{\text{wind}}(t)) = \text{const}\,,$$

and that $\alpha(0.5) = 1$.

The no-dump capacity is, consequently, determined according to:

$$P_{\text{nd}} = \min \frac{P_{\text{load}}(t)}{(r\, p_{\text{PV}}(t) + (1-r)\, p_{\text{wind}}(t))}\,,$$

The mismatch energy between renewable generation and load can be computed as:

$$P_{\text{mix}}(t) = \beta\, P_{\text{nd}}\, \alpha(r)\, \big(r\, p_{\text{PV}}(t) + (1-r)\, p_{\text{wind}}(t)\big) - P_{\text{load}}(t),$$

where β is a multiplier that enables oversizing the generation. Based on the values extracted from these empirical relationships, the model computes the optimal range of various parameters to ensure an optimal system efficiency that ultimately maximizes PV integration.

2. Storage utilisation and system-use index

I have introduced new and novel indices that identify the optimal system design parameters, and an optimal range of these parameters yields an optimal system performance. These indices provide deeper insights into the effectiveness of curtailment and storage integration within the broader energy infrastructure, enhancing the system's capacity to manage variability and optimize resource utilization.

The empirical relationship developed for defining the system boundaries is:

$$SU = \frac{-\sum(S(t) - S(t-\Delta t))}{S_{max}}, \qquad \text{if } S(t) < S(t-\Delta t)$$

The system-use index (SUI) is computed as follows:

$$\text{SUI} = \text{SU}\; k\; m\; u$$

where k, m and u are calculated by dividing annual energy discharge by the total consumed RE, average charging power by power capacity (PC), and total consumed RE by total RE generation, respectively:

$$k = \frac{-\sum(S(t) - S(t-\Delta t)}{\sum P_{useful}}, \qquad \text{if } (S(t) < S(t-\Delta t)$$

$$m = \frac{\sum S(t) - (S(t-\Delta t)}{P.C}, \qquad \text{if } (S(t) > S(t-\Delta t)$$

where $PC = {}^{S_{max}}/_{\Delta t_{full}}$

$$u = \frac{\sum P_{useful}}{\sum P_{rew}},$$

This approach enables me to create a novel and improved 3D visualization of the intricate relationships among these various interactive factors, providing a more comprehensive understanding of their interactions to improve PV integration.

3. Storage optimisation and its link to penetration

I have established clear boundaries of renewable penetration by linking them with storage type and application, resolving longstanding ambiguities in the literature. Through systematic analysis, I structured storage use into three distinct configurations, defined by their application and degree of penetration. This optimized categorization simplifies system design and modelling and provides actionable boundaries that overcome previous inconsistencies in renewable–dominated grid studies:

i. First configuration: This represents the no-dump capacity range–the threshold below which the system operates without requiring any form of storage or curtailment. While the exact no-dump capacity varies with the PV-wind mix, the maximum penetration achievable without storage or curtailment in the solar-only (PV) scenario is about 23.6%.

ii. Second configuration: Any increase in renewable penetration beyond this level necessitates storage and/or curtailment to manage fluctuations, enabling penetration up to 80%. Within this range, diurnal storage plays the key role in balancing short-term variability.

iii. Third configuration: Beyond 80% penetration, renewable deployment rises sharply even with slight increases in penetration. Thus, meeting the final 20% of demand presents a distinct challenge, which I addressed through seasonal storage capable of resolving long-term seasonal mismatches.

4. Maximizing the direct consumption of residential PV by imposing feed-in constraints

I have explored strategies for maximizing direct consumption of PV power in the low-voltage network. I have introduced a distinctive approach that proposes tailored grid-expansion and management solutions to enhance local network PV consumption. Building on this analysis, I have identified remarkably effective strategies that maximize the direct use of generated PV. The most efficient configuration combines a feed-in limit of 0.4–0.5 kW/kWp with battery storage capacities below 2 kWh/kWp, a setup that sharply reduces curtailment and achieves the highest levels of direct PV utilization.

Using the new approach – supported and validated with laboratory experiment – I have demonstrated that feed-in limits above 0.7 kW/kWp offer only negligible improvements in annual energy output. This confirms that the common practice of sizing inverters at 80–90% of the PV array capacity is not only economically inefficient but can also degrade system operation and power quality.

5. Addressing the data scarcity challenge in PV power forecasting

I found a practical solution to the data scarcity challenge in PV generation forecasting by developing a method that bridges satellite-derived and ground-measured data. Using a modified Z-score transformation, I have approximated satellite data to measured data based on their respective means and standard deviations. This approach enables the integration of widely available satellite data with the reliability of ground-based measurements by establishing a transparent empirical relationship, using transformation formulas derived from observed correlations. The resulting adjusted dataset is used to train the forecasting model. At the same time, testing is conducted on actual measured PV output, ensuring both accuracy and applicability in regions with limited monitoring infrastructure.

For each value in satellite-derived data, I found the standard normal form using the Z-score transformation (z):

$$z = \frac{P_{sat,i} - \mu_{sat}}{\sigma_{sat}} \qquad \text{and}$$

the rescaled satellite value ($P'_{sat,i}$) is determined to match the distribution of the measured data using:

$$P'_{sat,i} = z\,\sigma_{meas} + \mu_{meas}$$

where, $P_{sat,i}$, μ_{sat} and σ_{sat} are the hourly PV generation, mean, and standard deviation of the satellite-derived data, whereas, μ_{meas} and σ_{meas} are the mean and standard deviation of the measured data.

The proposed transformation has been rigorously validated against various well-established forecasting models. It demonstrates significant improvements in forecasting accuracy, achieving up to 24% in the LSTM-GRU model and 29.4% in the Informer model for six-step forecasts, based on RMSE metrics. For one-step predictions, the hybrid LSTM-GRU model yields a 43% increase in accuracy using the R^2 coefficient, confirming the effectiveness of the transformation approach. The method offers a scalable solution for regions with limited measurement infrastructure, reinforcing the role of satellite-based forecasting in advancing PV integration and shaping renewable energy policy development. Moreover, these forecasting improvements contribute to enhanced grid stability, optimize storage dispatch, and improve load balancing by offering flexibility to system operators.

The newly introduced methodological framework was validated against a well-established RL-based machine learning algorithm, showing negligible disparities. This strong agreement confirms the reliability of the framework and its underlying indices, reinforcing its accuracy and positioning it as a promising alternative for energy system optimization.

6. Impact of inverter loading on power quality

I have investigated the total harmonic characteristics of the PV inverter at various inverter loading conditions and I identified that inverter loading has a greater impact on the current total harmonic distortion (ThdI) than on the other power quality indicators. In heavily loaded inverters, ThdI remains relatively low, with only a few points exceeding the permissible limit of 5%. However, as the inverter load decreases, ThdI gradually exceeds this limit and rises further, reaching values of around 10%. The change in ThdI becomes more pronounced under lightly loaded conditions.

Accordingly, I have shown that the total current harmonic distortion (y) as a function of active power (P/P_{rated}) (x) for the three inverter loading conditions can be reliably estimated using a cubic polynomial model, achieving an R^2 value of 0.926.

$$y = 1.3546 + (-0.2973)\,x + (0.0239)\,x^2 + (-0.00063)\,x^3$$

The greater variation in ThdI observed in lightly loaded inverters implies that they are more sensitive to harmonic distortion when underutilized. Lightly and medium-loaded inverters exhibit higher variability per unit change in active power, whereas in heavily loaded conditions, inverter behaviour becomes more stable, likely because MPPT and control mechanisms operate more actively and consistently when PV generation is higher. By associating these distinct regression behaviours with specific sites, utilities can tailor inverter deployment strategies and better anticipate grid stress based on localized loading profiles.

This suggests oversizing an inverter for a given design can negatively impact power quality – not only cost – because an oversized inverter tends to operate predominantly under medium or light loading, where harmonic distortion is more pronounced. These findings highlight the need for inverter designs that ensure stronger control capability and more predictable interactions among power-quality parameters across varying load conditions.

5. CONCLUSION AND RECOMMENDATION

In this thesis, strategies have been investigated for maximizing PV integration into the power grid through three complementary approaches: large-scale PV deployment, residential PV integration, and PV generation forecasting and optimization.

To support large - scale PV integration, a novel methodological framework has been developed that flexibly captures the interactions between key system design parameters, such as storage capacity, storage duration, penetration, curtailment, wind-solar mix, and balancing requirements, while linking these parameters to a newly developed System–use index (SUI), which serves as a proxy of system efficiency. Various scenarios have been evaluated by fixing the PV share at 0%, 50%, and 100% of total RE capacity and applying different storage durations. Results show that penetration, curtailment, and storage all increase simultaneously; however, penetration gains diminish once storage or curtailment exceeds certain thresholds. Nevertheless, reaching 80–90% penetration is feasible with diurnal storage below 0.5 average daily demand with 6 hours of storage, alongside moderate curtailment. Achieving 100% renewable penetration is, however, challenging in the last 10–20% of the transition due to seasonal mismatches. Incorporating seasonal storage, about 8 average daily demand with a RE-to-load ratio of 1.2, enables complete decarbonization without balancing (back-up) needs. These findings highlight that an optimal mix of curtailment, storage, and wind-solar mix is essential for maximizing system efficiency, forming multidimensional constraints that are difficult to implement in existing techno-economic tools but critical for guiding policy development and regulation.

The role of residential PV in large-scale PV integration has been investigated by introducing a new concept of direct PV injection into low-voltage networks, overcoming the limitations of conventional self-sufficiency models. Findings reveal that imposing a feed-in limit and integrating battery storage significantly reduce curtailment, with a feed-in limit of 0.4 to 0.5 kW/kWp and battery storage below 2 kWh/kWp. This setup maximizes photovoltaic integration and enables renewable energy penetration of up to 30%. The study further examined the impact of inverter loading on power quality and found that highly loaded inverters operate more stably, while underutilized inverters exhibit significant distortion.

Machine learning based forecasting and optimization models have been proposed to maximize PV integration. To achieve this, a modified Z-score transformation and an RL model have been applied to align satellite-derived data with measured values to improve generation forecasting and optimize the system configuration. The findings reveal that the proposed transformation improves forecasting accuracy by up to 43%, demonstrating the effectiveness of the approach in providing a scalable solution for regions with limited measurement infrastructure.

These approaches collectively establish a comprehensive framework for addressing both system design and operational challenges in maximizing PV integration. By combining optimized PV–wind–storage configurations, effective residential PV deployment, and enhanced forecasting, the study provides valuable insights for achieving high levels of PV penetration in future renewable-dominated grids. Adopting, technical-first perspective, the study outlines multiple transition pathways by defining boundary conditions that can guide more detailed economic analyses and policy development. Furthermore, improved transmission planning and demand-side management will be essential for achieving more optimal system configurations and understanding parameter interactions. Incorporating more fine-tuned household data in residential PV analysis could further improve accuracy. This study emphasizes the importance of understanding the future renewable energy grid, using Eritrea as a case study; nevertheless, the methodology employed can be applied to a broader range of applications in a global perspective.

6. SUMMARY

MODELLING AND OPTIMIZATION OF LARGE-SCALE GRID-CONNECTED PHOTOVOLTAIC SYSTEMS WITH ENABLING TECHNOLOGIES

A holistic and innovative multifunctional simulation model is developed to maximize PV integration and offer a broader perspective on system design under interacting factors. Using hourly weather data from PVGIS and GWA, geographically distributed solar and wind sites in Eritrea were analysed to explore scenarios achieving 90% and beyond renewable penetration with and without storage. The results offer important insights of global importance by linking parameters in a uniquely broad way, while also addressing the context-specific requirements.

The analysis focuses on enabling large-scale PV integration through resource complementarity, energy storage, curtailment strategies, balancing capacity and improved forecasting, recognising that PV alone cannot capture full system complexity. Two new indicators, Storage Utilisation (SU) and SUI (SUI) are introduced to reveal the interactions between these variables. Results show that variable renewable penetration, curtailment and storage capacity increase simultaneously across all scenarios. The framework provides multiple options for combining storage and curtailment to achieve specific penetrations (including 100%), tailored to individual priorities and policy preferences, with the optimal approach lying in determining approximate optimal sizes to balance technical and economic feasibility.

Findings show that with a storage capacity below 0.5 of average daily demand, grid penetration exceeding 90% can be achieved while keeping curtailment under 20%, except in wind-only scenarios, which require higher curtailment. Diurnal storage manages short-term fluctuations and facilitates high renewable penetration of 80-90%, but its limitations become evident beyond this range. Meeting the final 10–20% of demand requires solutions beyond diurnal storage, as seasonal mismatches necessitate large storage and generation capacities. Incorporating seasonal storage of about 8 average daily demand with a RE-to-load ratio of 1.2 enables complete decarbonisation without balancing back-up needs. Overall, the study highlights that an optimal mix of curtailment, storage and wind–solar complementarity is essential for maximising system efficiency and for shaping policies and regulations that support deep decarbonisation.

Two additional approaches are introduced to maximise PV integration into the grid: expanding rooftop PV adoption (residential PV) and applying advanced PV generation forecasting. Using simulation techniques, the study examined the optimal deployment of residential PV and battery storage to boost PV penetration while minimising curtailment, applying a simple algorithm for PV injection, battery charging, and discharging. Key results show that imposing a feed-in limit and adding battery storage markedly cut curtailment, with limits of 0.4–0.5 kW/kWp and storage below 2 kWh/kWp giving the best outcomes. Furthermore, the study reveals that the power quality of grid-connected PV systems is strongly influenced by loading conditions, showing that highly loaded inverters maintain stable operation, while lightly loaded (underutilized) inverters exhibit increased distortion. The advantages of Effective PV forecasting for increasing renewable energy integration are studied, as it allows better management of generation and system operations. The new PV forecasting approach raises accuracy by up to 43%, enhancing generation management. When combined with resource complementarity and storage adoption, this improved forecasting strengthens grid stability, optimises scheduling, improves storage dispatch, reduces balancing needs, and boosts overall system efficiency, ultimately maximising renewable energy integration.

7. MOST IMPORTANT PUBLICATIONS RELATED TO THE THESIS

Refereed papers in foreign languages:

1. **Teklebrhan, N.**, Seres, I., Farkas, I. (2021): Matlab/Simulink-based modeling of grid-connected PV systems, *R&D in Mechanical Engineering Letters,* Vol**.** 21, pp. 5-13.
2. **Teklebrhan, N.**, Seres, I., Farkas, I. (2023): Large-scale Photovoltaic integration, *R&D in Mechanical Engineering Letters,* Vol. 24, pp. 199-222.
3. **Teklebrhan, N.**, Seres, I., Farkas, I. (2023): Energetic Complementarity of Solar PV and Wind Power Based on Satellite Data, European Energy Research Journal (2736-5506), Vol. 3, Issue 4, pp. 7-12, https://doi.org/10.24018/ejenergy.2023.3.4.97
4. **Teklebrhan, N.,** Solomon, A.A., Fredric. O., Erik. M., Seres, I., Farkas, I. (2025): Strategies for integrating residential PV and wind energy in Eritrea's electricity grid by imposing feed-in constraints in low voltage network, *Solar Energy,* vol. 286, https://doi.org/10.1016/j.solener.2024.113140 (Scopus: Q1, IF: 6.5)
5. **Teklebrhan, N.,** Nahom, W., Merhawi. G., Yemane, T., Seres, I., Farkas, I. (2025): Addressing photovoltaic (PV) forecasting challenges: Satellite-driven data models for predicting actual PV generation using hybrid (LSTM-GRU) model, *Energy Report,* Vol. 14, pp. 2141-2156, https://doi.org/10.1016/j.egyr.2025.08.034 (Scopus: Q1, IF: 5.1)
6. **Teklebrhan, N.,** Solomon, A.A., Fredric. O., Erik. M., Seres, I., Farkas, I. (2024): System design issues of high renewable energy systems, the case Eritrea, *Energy Policy*, Vol. xx(xx), pp. xxx. https://doi.org/xxxxx/xxxxxx *(*Scopus: D1: IF: 9.2) *(accepted)*
7. **Teklebrhan, N**., Solomon, A.A., Fredric. O., Erik. M., Seres, I., Farkas, I. (2025): System-level analysis of energy storage requirements for large-scale renewable integration, *Sustainable Energy Technology and Assessments* (Scopus: Q1, IF: 7) *(in progress)*

International conference proceedings

8. **Teklebrhan, N**., Seres, I., Farkas, I. (2022): Power Quality Issues in Grid-Connected PV systems (2022), 21th International Workshop for Young Scientists (BioPhys Spring 2022), Nitra, Slovakia, May 30- 3, 2022, pp. 77-78, ISBN 978-83-89969-74-3
9. **Teklebrhan, N**., Seres, I., Farkas, I. (2023): Maximizing large-scale PV integration employing enabling technologies, 29th Workshop on Energy and Environment, December 7-8, 2023, Gödöllő, Hungary, pp. 53–54. ISBN 978-963-623-079-1.
10. **Teklebrhan, N**., Seres, I., Farkas, I. (2024): The Role of Residential PV on Large Scale Photovoltaic Integration (2024), 23th International Workshop for Young Scientists (BioPhys Spring 2024), Lublin, Poland, May 23 – 24, 2024, pp. 106 -108, ISBN: 978-83-89969-88-0
11. **Teklebrhan, N**., Seres, I., Farkas, I. (2025): Renewable Synergy: A Holistic Approach to Power System Design in Eritrea, International Conference on Eritrean Studies (ICES2025), January 4-6, 2025, Asmara, Eritrea *(in progress)*.